Anharmonic effect on lattice distortion, orbital ordering and magnetic properties in Cs_2AgF_4

2009 J. Phys.: Condens. Matter 21 026014

(http://iopscience.iop.org/0953-8984/21/2/026014)

J. Phys.: Condens. Matter **21** (2009) 026014 (6pp) doi:10.1088/0953-8984/21/2/026014

Anharmonic effect on lattice distortion, orbital ordering and magnetic properties in Cs_2AgF_4

Da-Yong Liu[1,2], **Feng Lu**[1,2] **and Liang-Jian Zou**[1,3]

[1] Key Laboratory of Materials Physics, Institute of Solid State Physics, Chinese Academy of Sciences, PO Box 1129, Hefei 230031, People's Republic of China
[2] Graduate School of the Chinese Academy of Sciences, Beijing 100049, People's Republic of China

E-mail: zou@theory.issp.ac.cn

Received 5 September 2008, in final form 12 November 2008
Published 10 December 2008
Online at stacks.iop.org/JPhysCM/21/026014

Abstract

We develop the cluster self-consistent field method incorporating both electronic and lattice degrees of freedom to study the origin of ferromagnetism in Cs_2AgF_4. After self-consistently determining the harmonic and anharmonic Jahn–Teller distortions, we show that the anharmonic distortion stabilizes the staggered $x^2 - z^2/y^2 - z^2$ orbital and ferromagnetic ground state, rather than the antiferromagnetic one. The amplitudes of lattice distortions, Q_2 and Q_3, the magnetic coupling strengths, $J_{x,y}$, and the magnetic moment are in good agreement with the experimental observations.

(Some figures in this article are in colour only in the electronic version)

1. Introduction

Recently, the layered perovskite compound Cs_2AgF_4 containing the spin-1/2 $4d^9$ Ag(II) ion has attracted great interest, because it is isostructural to the high-T_c $3d^9$ Cu(II) cuprates. Cs_2AgF_4 was first refined to the tetragonal structure with the space group $I4/mmm$ in 1974 by Odenthal *et al* [1]. Very recently, however, McLain *et al* [2] found that the crystal structure is orthorhombic, with the space group $Bbcm$. The magnetic susceptibility and the inelastic neutron scattering experiments showed that this compound is well described as a two-dimensional (2D) ferromagnet (FM) with $T_c \sim 15$ K [2]. Further, McLain *et al* suggested that Cs_2AgF_4 is orbitally ordered at all temperatures of measurement, and the orbital ordering (OO) is responsible for the FM. These properties are in sharp contrast to the high-T_c parent La_2CuO_4 that is an antiferromagnetic (AFM) insulator. The microscopic origin of the unusual FM and OO in Cs_2AgF_4 attracts a lot of attention.

In Cs_2AgF_4, the basal plane consists of a 2D lattice of Jahn–Teller (JT) distorted AgF_6 octahedra with a pattern of alternating short and long Ag–F bonds. These analogous compounds with orbital degeneracy, such as Cs_2AgF_4 and K_2CuF_4, turn out to be 2D FM [2], while other compounds, such as K_2NiF_4 and Rb_2MnF_4, are AFM [3, 4]. Notice that the former with active JT ions leads to an orthorhombic structure, while the latter with nondegenerate orbitals only has a tetragonal structure. Although the difference between these two structures seems small, i.e. the main change is the position of the fluorine atoms in the basal plane, such a difference is of the utmost importance in leading to the distinct properties [5]. From early studies [6–9] in perovskite compounds, it is known that the anharmonic JT effect is a decisive factor for the orthorhombic crystal structure. To date, a lot of studies have been done for Cs_2AgF_4 utilizing the density functional theory [10–15]; however, few authors focus on the anharmonic JT effect on the lattice, OO and FM ground-state properties in Cs_2AgF_4.

Previous studies in the analogous compound K_2CuF_4 have provided us with two distinct scenarios for the FM and OO ground state. On the one hand, Kugel and Khomskii showed that the cooperative JT effect, especially the anharmonic JT effect [16], plays a key role in stabilizing the OO ground state in K_2CuF_4. On the other hand, to resolve the difficulty of the Kugel–Khomskii (KK) electronic superexchange (SE) coupling model [17], which is usually suitable for the Mott–

[3] Author to whom any correspondence should be addressed.

Hubbard insulators with $U_d < \Delta$ (here U_d is the on-site Coulomb repulsion and Δ is the charge-transfer energy), and to address the FM and OO ground state, Mostovoy and Khomskii [18] proposed a modified SE coupling model, which is suitable for the charge transfer insulating K_2CuF_4 with $U_d > \Delta$. Obviously, to understand the unusual ground-state properties, such as the lattice, orbital and magnetic properties in K_2CuF_4 and Cs_2AgF_4, one should incorporate the cooperative JT effect [19] and the anharmonic JT effect into the charge-transfer SE interactions.

To treat these strongly correlated systems more precisely, based on the cluster self-consistent field approach developed previously [20], we explicitly take into account the orthorhombic JT distortions and the charge-transfer SE interactions, in which spin order, OO and lattice distortion are determined self-consistently. We show that, driven by a strong anharmonic effect and Hund's coupling, Cs_2AgF_4 has a much more stable ferromagnetic ground state. The theoretical amplitudes of lattice distortions, Q_2 and Q_3, the magnetic coupling strengths, $J_{x,y}$, and the magnetic moment are in good agreement with the experimental observation in Cs_2AgF_4.

This paper is organized as follows: an effective Hamiltonian and the cluster self-consistent field (SCF) approach are described in section 2; then the results and discussions of the lattice structure and distortions, orbital ordering and magnetic properties in Cs_2AgF_4 are presented in section 3; section 4 is devoted to remarks and the summary.

2. Model Hamiltonian and method

An effective 2D Hamiltonian in Cs_2AgF_4 including both the SE and the JT couplings is written

$$H = H_{QJT} + H_{SE} \tag{1}$$

where H_{SE} describes the effective SE couplings; H_{QJT} describes the JT couplings associated with the electron and the lattice distortion. Note that spin, orbital and lattice degrees of freedom couple to each other in Hamiltonian (1). The JT effect associated with one hole per Ag^{2+} site in the AgF_4 sheets reads [19]

$$H_{QJT} = g\sum_i \left(Q_{i2}\tau_i^x + Q_{i3}\tau_i^z\right) + \frac{K}{2}\sum_i \left(Q_{i2}^2 + Q_{i3}^2\right) + G\sum_i \left[\left(Q_{i3}^2 - Q_{i2}^2\right)\tau_i^z - 2Q_{i2}Q_{i3}\tau_i^x\right] \tag{2}$$

where both the linear and the quadratic vibronic coupling terms have been included. The first and second terms describe the linear harmonic JT effect. The third one, i.e. the quadratic coupling, arises from the anharmonic JT effect and contributes to the anisotropic energy [16, 19]. Here Q_{i2} and Q_{i3} are the normal vibration coordinates, defined as $Q_2 = (-X_1 + X_2 + Y_3 - Y_4)/2$ and $Q_3 = (-X_1 + X_2 - Y_3 + Y_4 + 2Z_5 - 2Z_6)/\sqrt{12}$ [21], with X, Y and Z being the coordinates of the ith F ions. g is the linear JT coupling strength, G is the coefficient of quadratic coupling, and K is the elastic constant. For Cs_2AgF_4, we fix $K = 10$ eV Å^{-2} throughout this paper.

Since Cs_2AgF_4 is a strongly correlated charge-transfer insulator [11], the 2D SE interactions between 4d orbitals of Ag^{2+} ions through 2p orbitals of F atoms are described [18]:

$$H_{SE} = \sum_{\substack{i,\alpha \\ \alpha=x,y}} \left[(J_1 + J_2 I_i^\alpha + J_3 I_i^\alpha I_{i+\alpha}^\alpha)\vec{S}_i \cdot \vec{S}_{i+\alpha} + J_4 I_i^\alpha + J_5 I_i^\alpha I_{i+\alpha}^\alpha\right], \tag{3}$$

where the operator $\vec{S}_i$ denotes the $S = 1/2$ spin at site i, and $I_i^\alpha = \cos(2\pi m_\alpha/3)\tau_i^z - \sin(2\pi m_\alpha/3)\tau_i^x$, which is a combination of the components of the orbital operators $\vec{\tau}$. $\alpha = x, y$, and $(m_x, m_y) = (1, 2)$, denote the direction of a bond in the AgF_4 sheets. In equation (3), the coupling coefficients J_n (n = 1–5), read

$$J_1 = t^2\left[1/U_d + 2/(2\Delta + U_p) - J_H/(2U_d^2)\right],$$

$$J_2 = 4t^2\left[1/U_d + 2/(2\Delta + U_p)\right],$$

$$J_3 = 4t^2\left[1/U_d + 2/(2\Delta + U_p) + J_H/(2U_d^2)\right],$$

$$J_4 = t^2\left[2/\Delta - 1/U_d - 2/(2\Delta + U_p)\right]$$

and

$$J_5 = t^2\left[1/U_d + 2/\Delta - 2/(2\Delta + U_p) + 3J_H/(2U_d^2)\right]$$

with $t = t_{pd}^2/\Delta$, respectively. Here Δ is the electron-transfer energy between silver 4d and fluorine 2p orbitals, U_d and U_p are the Coulomb repulsion energies on Ag and F, respectively, and J_H is the Hund's coupling on Ag. Note that the coefficients may be positive and negative, thus the AFM and the FM components coexist in J_n. Since the 4d orbitals of Ag^{2+} ions are less localized than the 3d orbitals of Cu^{2+} ions in K_2CuF_4, the Coulomb repulsion U_d of the Ag^{2+} ion is about 3–5 eV, and J_H ranges from 0.1 to 0.5 eV, in accordance with the LDA + U results [10, 11, 15]. In general, the Coulomb repulsion U_p is about 5 eV in F^-. The charge-transfer energy Δ is roughly estimated from the difference of the centers of gravity between the 4d and 2p levels in band structures, which also allows us to estimate t_{pd} from the bandwidth of the electronic structures available [4, 10, 15], $\Delta = U_d - 2$ eV, and $t_{pd} \simeq 0.6$ eV.

In such a strongly correlated spin–orbital–lattice system, according to the Feynman–Hellman theorem, the ground state energy is minimized with respect to Q_{i2} and Q_{i3}, i.e.,

$$\left\langle \frac{\partial H}{\partial Q_{i2}} \right\rangle = 0, \qquad \left\langle \frac{\partial H}{\partial Q_{i3}} \right\rangle = 0.$$

From this one could find that the strength of the normal modes and the lattice distortion critically depend on the orbital polarization through the following equations:

$$\langle Q_{i2}\rangle = g\frac{K\langle\tau_i^x\rangle + 4G\langle\tau_i^x\rangle\langle\tau_i^z\rangle}{4G^2(\langle\tau_i^x\rangle^2 + \langle\tau_i^z\rangle^2) - K^2}$$
$$\langle Q_{i3}\rangle = g\frac{K\langle\tau_i^z\rangle + 2G(\langle\tau_i^x\rangle^2 - \langle\tau_i^z\rangle^2)}{4G^2(\langle\tau_i^x\rangle^2 + \langle\tau_i^z\rangle^2) - K^2}. \tag{4}$$

Notice that, in the absence of the anharmonic JT effect ($G = 0$), $\langle Q_{i2}\rangle \sim -(g/K)\langle\tau_i^x\rangle$ and $\langle Q_{i3}\rangle \sim$

$-(g/K)\langle\tau_i^z\rangle$. To obtain the amplitude of the lattice distortion, one should determine the spin, the orbital and the deformation configurations self-consistently.

In order to treat the spin–orbit correlations and fluctuations with high accuracy in a strongly correlated system, the cluster-SCF approach [20] developed previously is applied to the spin–orbital Hamiltonian (1). The cluster-SCF approach includes the exact treatment of the interactions inside the cluster, and the self-consistent field treatment of the interactions between the cluster and the surrounding environment. The main procedure is briefly outlined as follows. First, we choose a cluster consisting of four Ag^{2+} ions. The ith site is surrounded by two Ag sites inside the cluster and two Ag sites outside the cluster, which provide two internal interactions and two external SCF fields, respectively. Thus, the effective Hamiltonian of the cluster reads

$$h_{\rm cluster} = \sum_{\substack{i,\alpha \\ \alpha=x,y}} \left[\left(J_1 + \frac{J_2}{2}(I_i^\alpha + I_{i+\alpha}^\alpha) + J_3 I_i^\alpha I_{i+\alpha}^\alpha \right) \vec{S}_i \cdot \vec{S}_{i+\alpha} + J_4 I_i^\alpha + J_5 I_i^\alpha I_{i+\alpha}^\alpha \right] + g \sum_i (Q_{i3}\tau_i^z + Q_{i2}\tau_i^x) + G \sum_i \left[(Q_{i3}^2 - Q_{i2}^2)\tau_i^z - 2Q_{i2}Q_{i3}\tau_i^x \right] + \frac{K}{2} \sum_i (Q_{i2}^2 + Q_{i3}^2) + \sum_i h_i^{\rm scf} \quad (5)$$

with the SCF $h_i^{\rm scf}$ contributing from the j'th external site interacting with the ith internal site through $H_{ij'}$, $h_i^{\rm scf} = {\rm Tr}_{j'}(\rho_{j'} H_{ij'})$, where $\rho_{j'}$ denotes the reduced density matrix of the j'th site, and i runs over all sites inside the cluster. We first substitute the spin coupling $\vec{S}_i \cdot \vec{S}_{i+\alpha}$ into the cluster Hamiltonian with the initial spin correlation function $\langle \vec{S}_i \cdot \vec{S}_{i+\alpha} \rangle$, and diagonalize the orbital part of the cluster Hamiltonian (5) in the presence of the orbital SCF. The orbitalization $\langle \vec{\tau} \rangle$ and the orbital correlation functions $\langle \vec{\tau}_i \cdot \vec{\tau}_{i+\alpha} \rangle$ are thus obtained. Then, we substitute the orbital operator and the orbital couplings with $\langle \vec{\tau} \rangle$ and $\langle \vec{\tau}_i \cdot \vec{\tau}_{i+\alpha} \rangle$ into $h_{\rm cluster}$, and diagonalize the spin part of the cluster Hamiltonian in the presence of the spin SCF. Hence, we obtain a set of new averaged spin $\vec{S}_i$ and spin correlation functions $\vec{S}_i \cdot \vec{S}_{i+\alpha}$. We repeat the above steps until the ground-state energy and the spin and orbital correlation functions converge to the accuracies. From the stable spin–orbital ground state, one could get the magnetic coupling strengths J_x and J_y through $J_\alpha = J_1 + J_2\langle I_i^\alpha \rangle + J_3 \langle I_i^\alpha I_{i+\alpha}^\alpha \rangle$; here $\alpha = x, y$. The advantage of our approach over the traditional mean-field method is that the short-range spin and orbital correlations as well as the quantum fluctuations are taken into account properly, especially in the low-dimensional systems.

3. Results and discussion

In this section, we present the numerical results of the ground state of the charge-transfer insulator Cs_2AgF_4 within the cluster-SCF approach. We mainly discuss the role of the anharmonic effect on lattice structure and distortions, orbital ordering and magnetic properties in the ground state.

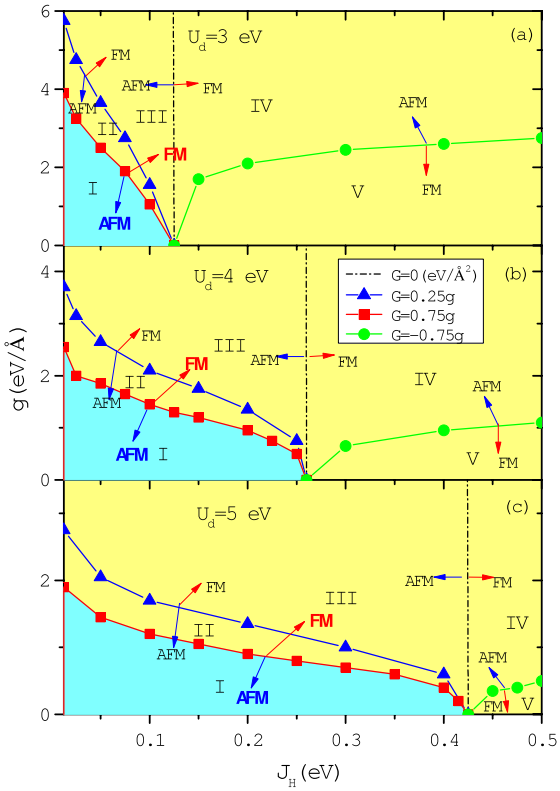

Figure 1. Phase diagrams of JT coupling g versus Hund's coupling $J_{\rm H}$ in Cs_2AgF_4 for different Coulomb repulsions, (a) $U_{\rm d} = 3$ eV, (b) $U_{\rm d} = 4$ eV and (c) $U_{\rm d} = 5$ eV. The solid circles, dashed line, solid triangles and solid squares denote the FM/AFM phase boundaries for the anharmonic coupling $G = -0.75g$, 0, $0.25g$ and $0.75g$, respectively. G is in the unit of eV Å^{-2}.

3.1. Ground-state phase diagram

To clarify the roles of the SE coupling and the JT effect in the origin of the FM, we first perform numerical calculations with equation (5) and obtain the g–$J_{\rm H}$ phase diagram, as shown in figure 1. Since the on-site Coulomb interaction $U_{\rm d}$ in Cs_2AgF_4 is not well defined, we present the g–$J_{\rm H}$ phase diagram for $U_{\rm d} = 3$, 4 and 5 eV in figures 1(a), (b) and (c), respectively. Accordingly, we find that the anharmonic distortion strength G plays a very important role in the phase diagram. With the variation of G from negative to positive via zero, the FM–AFM phase boundaries exhibit critical changes. As we see in figure 1(a), at $G = -0.75g$, the stable ground-state phase in regions I–IV is AFM, while that in region V is FM; at $G = 0$, a vertical line separates the AFM ground state in regions I–III from the FM one in regions IV–V; when the anharmonic distortion strength G becomes positive, more regions become FM ordering; at $G = 0.75g$, only the ground state in region I is AFM. Figures 1(b) and (c) qualitatively resemble figure 1(a).

The competitive FM and AFM couplings in the SE Hamiltonian result in the FM phase for large $J_{\rm H}$ and the AFM phase for small $J_{\rm H}$. As we expect in figures 1(a)–(c), strong Coulomb repulsion favors the AFM phase, hence the AFM regime becomes large with the increase of $U_{\rm d}$. Besides the fact that strong Hund's coupling $J_{\rm H}$ favors the FM phase, the large anharmonic JT effect also favors the FM

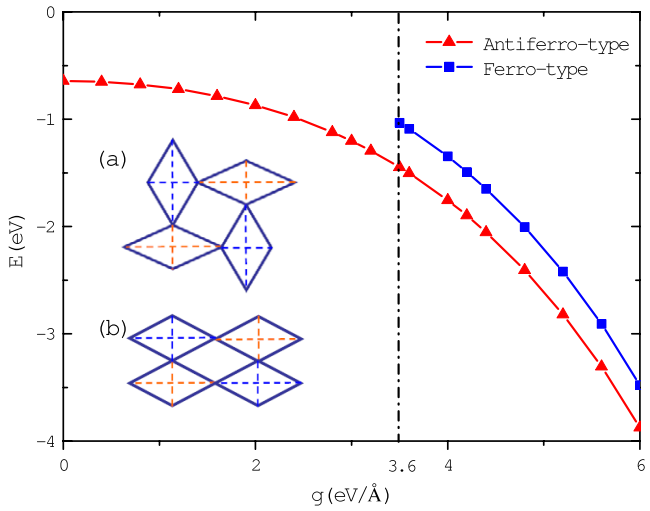

Figure 2. Dependence of ground-state energy on the JT coupling strength with $G = 0.75g$ in the antiferro-type (a) and the ferro-type (b) distortions in the AgF_4 plaquette. The dashed vertical line indicates the appearance of the ferro-type distortion. Theoretical parameters: $U = 3$ eV and $J_H = 0.3$ eV.

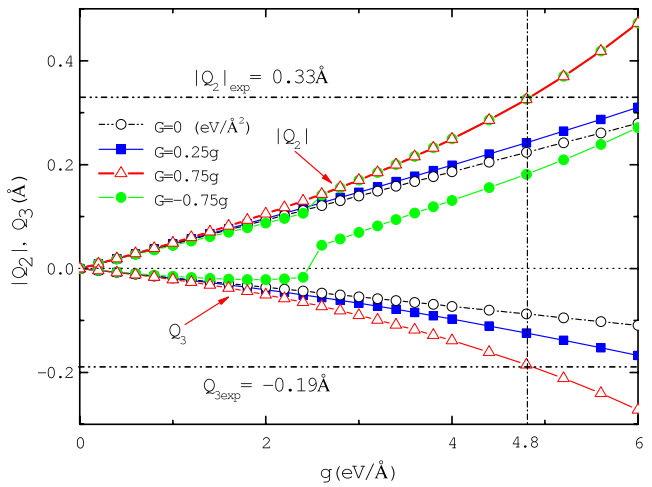

Figure 3. The amplitudes of $|Q_2|$ and Q_3 as a function of the JT coupling with different G. Two dashed horizontal lines correspond to the experimental values of $|Q_2|$ and Q_3; the vertical dashed line indicates the linear JT coupling $g = 4.8$ eV Å^{-1} for $G = 0.75g$ in Cs_2AgF_4. The other parameters are the same as figure 2.

ground state. Therefore, the complete consideration of the realistic interactions in equation (1) most probably leads to the FM ground state in Cs_2AgF_4. Moreover, from the recent first-principles electronic calculations, the Coulomb repulsion between Ag 4d electrons is about 3 eV [10]. We expect that the Hund's coupling J_H lies in the range 0.1–0.3 eV, so that the interaction parameters of Cs_2AgF_4 fall in the FM region in the phase diagram.

Experimentally, it is hard to determine the sign of the anharmonic coupling strength G in Cs_2AgF_4. From figure 1, it is seen that when the positive anharmonic effect is very large the ground state stabilizes in the FM phase even in the absence of Hund's coupling. Therefore, the positive anharmonic coupling most favors the FM ground state. In contrast, for $G < 0$, due to the SE coupling, the ground state is FM when the harmonic JT coupling strength g is small; however, when g becomes large, the anharmonic coupling favors the AFM ground state. Thus, considering the strong JT effect in Cs_2AgF_4, one expects that G is most probably positive, which will be further confirmed in the lattice distortion, the orbital ordering and the magnetic properties in what follows.

3.2. Lattice structure and distortions

Different from La_2CuO_4, the unusual FM and the orthorhombic structure of Cs_2AgF_4 is the result of the interplays of the spin, orbital and lattice degrees of freedom, especially the contribution of the anharmonic JT effect. The normal coordinates Q_2 and Q_3 of the JT distortions in Cs_2AgF_4 are obtained self-consistently through equations (4) and (5). We find that for positive and large G the structural distortion in the ground state is antiferro-type (Q_2, Q_3; $-Q_2$, Q_3), corresponding to the alternative short and long bonds in the AgF_4 plaquette. However, the ground-state energy of the ferro-type (Q_2, Q_3; Q_2, Q_3) distortion is higher than that of the antiferro-type distortion, as shown in figure 2, and the ferro-type distortion only appears in the strong JT region because of its instability in this system.

Notice that the experimentally observed lattice structure has the antiferro-type distortion with the long and short Ag–F bond lengths of 2.441 and 2.111 Å in the AgF_4 plaquette [2]; one can deduce the corresponding distortions $Q_2 \approx 0.33$ Å and $Q_3 \approx -0.19$ Å. Theoretically, through the self-consistent numerical calculations, we obtain the amplitudes of the Q_2 and the Q_3 distortions in Cs_2AgF_4 with the variation of the JT coupling for different anharmonic coupling parameters, as shown in figure 3. When the linear JT coupling strength g is about 4.8 eV Å^{-1} at $G = 0.75g$, the theoretical distortions are $|Q_2| \approx 0.33$ Å and $Q_3 \approx -0.19$ Å (see the dashed vertical line in figure 3), in good agreement with the corresponding experimental observation in Cs_2AgF_4 [2]. Meanwhile, we find that a positive G leads to a negative Q_3, giving rise to the correct distortion $c/a = 2s/(l + s) < 1$ in orthorhombic Cs_2AgF_4. However, a negative G gives a positive Q_3, resulting a wrong distortion $c/a = 2l/(l + s) > 1$. All the other analogous substances without JT ions, e.g. K_2NiF_4, K_2MnF_4 [3, 4], are tetragonal, rather than the orthorhombic symmetry in Cs_2AgF_4 with JT ions. In fact, it is the positive anharmonic effect that lowers the lattice symmetry, leading to the compression of the ligand octahedron along the c-axis [22, 23].

3.3. Orbital ordering

The unusual FM and distinct orthorhombic structure in Cs_2AgF_4 are in fact associated with the formation of the long-range OO, as shown by a few authors recently utilizing first-principles calculations [10, 11, 13, 15]. Our study also confirms this point. Furthermore, we demonstrate that the anharmonic effect plays an essential role in the OO properties of Cs_2AgF_4. In general, one can describe the orbital occupied

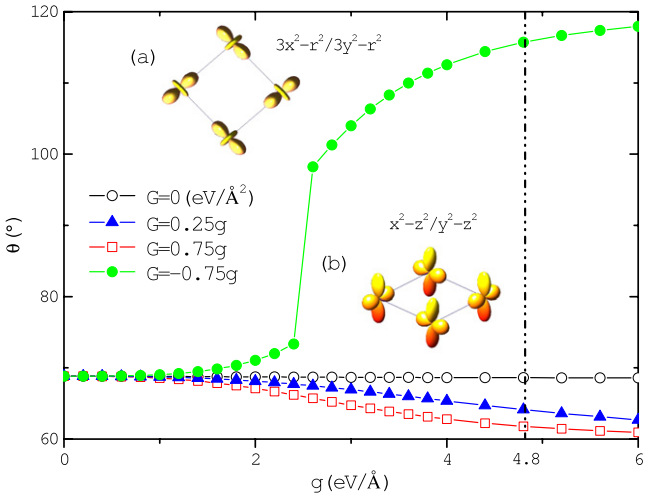

Figure 4. Orbital angle as a function of the JT coupling with different anharmonic couplings. Insets (a) and (b) correspond to the $3x^2 - r^2/3y^2 - r^2$ and $x^2 - z^2/y^2 - z^2$ orbital orders for large negative and positive G values, respectively. The vertical dashed line corresponds to the case of $g = 4.8$ eV Å^{-1} for Cs_2AgF_4. The other parameters are the same as figure 2.

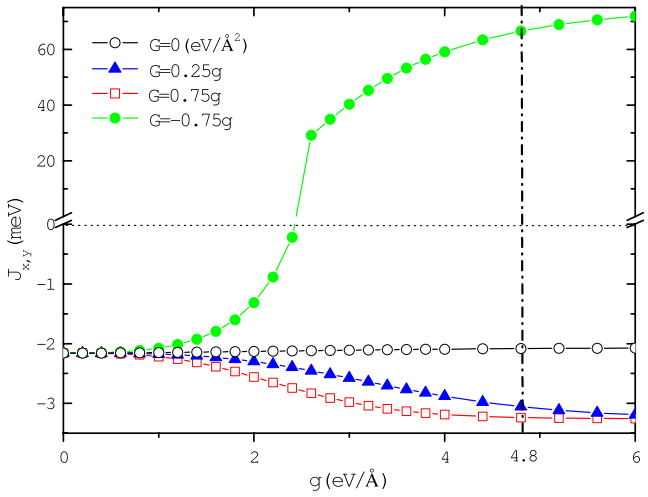

Figure 5. Magnetic coupling strengths $J_{x,y}$ in the AgF_4 plaquette as a function of the JT coupling with different anharmonic couplings. The vertical dashed line corresponds to the case of $g = 4.8$ eV Å^{-1} for Cs_2AgF_4. The other parameters are the same as figure 2.

state of each site in terms of $|\phi\rangle = \cos\frac{\theta}{2}|3z^2 - r^2\rangle \pm \sin\frac{\theta}{2}|x^2 - y^2\rangle$ with the orbital angle θ. Here '±' refers to the two sublattices of the antiferro-distortion in the AgF_4 plaquette. Figure 4 shows the orbital angle θ as a function of the linear JT coupling strength g with different anharmonic couplings G. The role of the anharmonic coupling in the orbital angle, hence the OO, is clearly seen. For strong JT distortion and $G = 0.75g$, the OO is staggered $z^2 - x^2/z^2 - y^2$; see inset (b) in figure 4. The orbital angle obtained is about 61.8° for $g = 4.8$ eV Å^{-1}, as indicated by the dashed vertical line in figure 4, which is consistent with the experimental suggestion for Cs_2AgF_4 [2]. This is different from the case in La_2CuO_4, where the distance between apical O and Cu is much larger than that in the a–b plane, resulting in the pure $3z^2 - r^2$ hole orbitals. Notice that the orbital angle is also close to 60° in the ferro-type solution. However, it is the ferro-orbital $z^2 - x^2/z^2 - x^2$ or $z^2 - y^2/z^2 - y^2$ symmetry rather than the staggered antiferro-orbital $z^2 - x^2/z^2 - y^2$ symmetry in the antiferro-type solution.

As a comparison, for $G < 0$, the orbital angle $\theta > \pi/2$; as $|G|$ becomes very large, $\theta \to 2\pi/3$, and the holes occupy the $d_{3x^2-r^2}/d_{3y^2-r^2}$ orbitals in an orderly way, as seen in inset (a) in figure 4. For $G = 0$, however, the orbital angle is nearly constant with the increase of the linear JT coupling g, giving rise to $\theta = 68°$. Note that in the absence of the anharmonic effect the SE couplings contribute to the same OO as the harmonic JT effect does. In this situation, the orbital configuration is characterized by orbital angle θ_0: $\tan\theta_0 = Q_{i2}/Q_{i3}$ [19]. Then $Q_{i2}/Q_{i3} \sim \tau_i^x/\tau_i^z$, which is almost independent of the linear coupling g, indicating that the linear JT coupling has little influence on the orbital angle in the absence of the anharmonic effect. This also shows the key role of the anharmonic effect in the OO from the other aspect. In addition, we find that the orbital angle is nearly unchanged with the Hund's coupling J_H. This result can be easily understood, since the orbital angle is mainly determined by the 'orbital field' corresponding to the J_4 term in H_{SE}, which is independent of J_H [18].

3.4. Magnetic properties

The magnetic properties are also strongly influenced by the anharmonic effect, as shown in figure 5. In the present situation, we find that the difference between J_x and J_y is negligible. From figure 5, one finds that in the absence of the anharmonic effect ($G = 0$), due to the SE coupling, the magnetic couplings between Ag spins are FM, and nearly remain unchanged with the increasing of g, while for $G < 0$, due to the SE coupling, the magnetic coupling between Ag ions is FM at small g. With the increase of the JT effect, the magnetic couplings between Ag ions, $J_{x,y}$, vary from FM to AFM, which is in contradiction with Cs_2AgF_4. For $g = 4.8$ eV Å^{-1} and $G = 0.75g$, as denoted by the dashed vertical line in figure 5, the magnetic couplings in the AgF_4 plaquette, i.e. $J_{x,y}$, are about −3.3 meV, very close to the experimental values, −3.793 to −5.0 meV [2]. The agreement between the present magnetic coupling strengths and the experimental observation is much better than those inferred from the first-principles electronic structure calculations [13, 14].

This result, combining those of the lattice distortion and the orbital angle, is in accordance with the Goodenough–Kanamori–Anderson rules [24]. Also in figure 5, one notices that in the presence of strong anharmonic coupling G the FM coupling strength increases with the linear JT coupling g. Therefore, the FM couplings in Cs_2AgF_4 further verify the key role of the anharmonic effect in the ground-state properties. In addition, the calculated magnetic moment is about 1 μ_B, which approaches the classical value and is comparable to the experimental data observed in a muon-spin relaxation experiment [25]. This is a classical value of the Ag ion, in

comparison with the experimental value 0.8 μ_B at 5 K [2]. The reduction of the experimental magnetic moment may originate from three factors: the presence of non-magnetic impurity phases and the covalence effects as pointed out by McLain *et al* in [2], as well as the AFM fluctuations between AgF_4 layers. We expect that the weak interlayer AFM interaction and the covalency effect, which are neglected in the present 2D model, contribute to the major part of the reduction of the magnetic moment of Ag spins.

4. Remarks and summary

As we have shown in the preceding sections, the anharmonic JT effect incorporating the SE coupling drives the 4d orbitals of Cs_2AgF_4 into the $d_{z^2-x^2}/d_{z^2-y^2}$ ordering, rather than the $d_{3z^2-r^2}$ orbital ordering in La_2CuO_4. Consistent with the Goodenough–Kanamori–Anderson rules [24], the ground state of Cs_2AgF_4 is unusual, FM insulating with the orthorhombic structure, different from the *Néel* AFM insulating ground state with the tetrahedral structure in La_2CuO_4. Our results preclude the possibility of the FM ground state originating from the covalency effect [12]. One consequence of such a difference is that the electron or hole doping in La_2CuO_4 leads to strong AFM fluctuations, which may contribute to the Cooper-pairing glue for the high-T_c superconductivity. We anticipate that the electron doping in Cs_2AgF_4 will lead to weak FM fluctuation, though it will not contribute to the same SC mechanism as the cuprate superconductors.

Notice that in the present intermediate correlated and charge-transfer insulator the 2D effective SE interactions incorporating the JT couplings underestimate the covalency effect between Ag 4d and F 2p orbitals. The covalency effect between Ag and F ions can be well considered within the first-principles electronic structure calculations [10, 12, 14, 15]. On the other hand, once the JT distortion occurs, the hopping integrals, $t_{x,y}$, between Ag ions are slightly different in different crystallographic axes. We expect that this change will not significantly modify our results quantitatively.

In summary, an effective model Hamiltonian with spin, orbital and lattice degrees of freedom coupling to each other allows us to self-consistently describe the lattice structure change, orbital ordering and magnetic coupling properties, etc. Driven by the JT distortion, especially by the anharmonic effect, Cs_2AgF_4 stabilizes in the 2D FM ground state. The correct lattice structure, orbital ordering and magnetic coupling observed experimentally can also be addressed in the present theoretical framework.

Acknowledgments

This work was supported by the NSFC of China No 90303013 and 10874186, the BaiRen Project, and the Knowledge Innovation Program of the Chinese Academy of Sciences. Some of the calculations were performed at the Center for Computational Science of CASHIPS and the Shanghai Supercomputer Center.

References

[1] Odenthal R-H, Paus D and Hoppe R 1974 *Z. Anorg. Allg. Chem.* **407** 144
[2] McLain S E, Dolgos M R, Tennant D A, Turner J F C, Barnes T, Proffen T, Sales B C and Bewley R I 2006 *Nat. Mater.* **5** 561
[3] Goodenough J B 1963 *Magnetism and the Chemical Bond* (New York: Interscience)
[4] García J M, Aramburu J A, Barriuso M T and Moreno M 2004 *Phys. Rev. Lett.* **93** 226402
[5] Grochala W 2006 *Nat. Mater.* **5** 513
[6] Sakamoto N 1982 *Phys. Rev.* B **26** 6438
[7] Bates C A 1978 *Phys. Rep.* **35** 187
[8] Muramatsu S and Iida T 1970 *J. Phys. Chem. Solids* **31** 2209
[9] Bacci M, Ranfagni A, Fontana M P and Viliani G 1975 *Phys. Rev.* B **11** 3052
[10] Wu H and Khomskii D I 2007 *Phys. Rev.* B **76** 155115
[11] Kasinathan D, Koepernik K, Nitzsche U and Moudden H 2007 *Phys. Rev. Lett.* **99** 247210
[12] Kasinathan D, Kyker A B and Singh D J 2006 *Phys. Rev.* B **73** 214420
[13] Hao X F, Xu Y H, Wu Z J, Zhou D F, Liu X J and Meng J 2007 *Phys. Rev.* B **76** 054426
[14] Dai D, Whangbo M-H, Köhler J, Hoch C and Villesuzanne A 2006 *Chem. Mater.* **18** 3281
[15] Kan E J, Yuan L F, Yang J L and Hou J G 2007 *Phys. Rev.* B **76** 024417
[16] Khomskii D I and Kugel K I 1973 *Solid State Commun.* **13** 763
[17] Kugel K I and Khomskii D I 1973 *Sov. Phys.—JETP* **37** 725
[18] Mostovoy M V and Khomskii D I 2004 *Phys. Rev. Lett.* **92** 167201
[19] Kanamori J 1960 *J. Appl. Phys.* **31** 14S
[20] Chen D-M and Zou L-J 2007 *Int. J. Mod. Phys.* B **21** 691
[21] Van Vleck J H 1939 *J. Chem. Phys.* **7** 72
[22] Kugel K I and Khomskii D I 1982 *Sov. Phys.—Usp.* **25** 231
[23] Khomskii D and van den Brink J 2000 *Phys. Rev. Lett.* **85** 3329
[24] Goodenough J B 1955 *Phys. Rev.* **100** 564
Kanamori J 1959 *J. Phys. Chem. Solids* **10** 87
Anderson P W 1959 *Phys. Rev.* **115** 2
[25] Lancaster T, Blundell S J, Baker P J, Hayes W, Giblin S R, McLain S E, Pratt F L, Salman Z, Jacobs E A, Turner J F C and Barnes T 2007 *Phys. Rev.* B **75** 220408(R)